Langmuir

Article

pubs.acs.org/Langmuir

Interaction Forces between Ternary Lipid Bilayers Containing Cholesterol

James Kurniawan,[†] Nai-Ning Yin,[‡] Gang-yu Liu,[‡] and Tonya L. Kuhl*[,†]

[†]Department of Chemical Engineering and Materials Science and [‡]Department of Chemistry, University of California—Davis, Davis, California 95616, United States

ABSTRACT: Interaction force−distance profiles between substrate-supported membranes composed of equimolar ternary mixtures of unsaturated phosphotidylcholine (PC) lipid, saturated PC lipid, and cholesterol were determined using the surface force apparatus. Both double and single unsaturated PC lipids were studied. In all cases, the membranes were slightly negatively charged, resulting in a weak, long-range electrostatic repulsion. Corroborative atomic force microscopy, zeta potential, and fluorescence microscopy measurements were used to establish that a small level of charged lipid impurities (∼1/400 lipid molecules) were responsible for the repulsive electrostatic interaction between the membranes. At contact, the membranes were adhesive. The magnitude of the adhesion was greater than the van der Waals interaction between pure PC membranes without cholesterol. The enhanced adhesion was primarily attributed to hydrophobic attraction due to the presence of nanoscopic membrane defects which exposed the underlying membrane leaflet. The interaction force−distance profiles also demonstrated that the nanoscopic defects enabled membrane restructuring in the contact region.

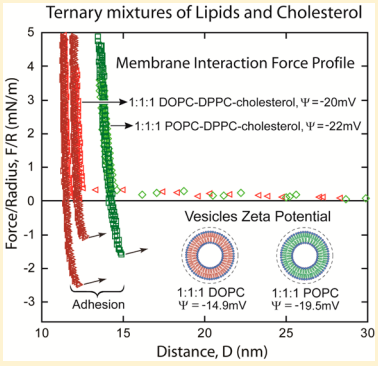

INTRODUCTION

Biological membranes are complex, self-organized structures that define boundaries and compartmentalize volumes in living matter. Composed primarily of cholesterol and a wide variety of lipid and protein molecules, a typical mammalian membrane contains hundreds of different constituent molecules. Biophysical studies seek to recapitulate the fundamental thermodynamic and physical attributes of biological membranes using simpler systems of a few components with well-defined compositions. Importantly, model systems still exhibit a variety of properties and different ordered states ranging from the tightly packed gel phase to the fluidlike liquid ordered (L_o) and liquid disordered (L_d) phases. Although binary lipid mixtures can display a coexistence of gel and fluid phases, cholesterol is necessary for L_d and L_o fluid-phase coexistence.[1,2] Lateral heterogeneities within model membranes have been widely used to study lipid domain formation and as analogues for lipid rafts.[3,4] In particular, the phase behavior of ternary mixtures of saturated lipids, unsaturated lipids, and cholesterol is considered to be the simplest model of biological membranes insofar as their fluidity and coexistence of L_d and L_o phases.[5−7] As a result, there have been a plethora of studies focused on elucidating the specific interactions and condensed complexes of cholesterol−lipid mixtures, including a determination of ternary phase diagrams and alterations of membrane mechanical properties on the macroscale[8−12] and temporal composition fluctuations and the preferential segregation of different membrane constituent moieties on the nanoscale.[13,14] However, less is known regarding how the presence of cholesterol modifies the interactions between membranes.

A majority of investigations of ternary mixtures have focused on monolayers at the air−water interface or on unilamellar vesicles in solution.[3−7] In both cases, the incorporation of lipid-based dyes enables the use of fluorescence microscopy (FM) to measure domains as a function of surface pressure, composition, and temperature.[6,7] Similar investigations with substrate-supported membranes can be carried out and also allow for atomic force microscopy (AFM) measurements of domain height or frictional differences due to alterations in the packing and composition of the domains. More detailed thermodynamic information including the elucidation of tie lines in the two-phase region has been extracted from NMR and X-ray scattering measurements.[7]

In this work, we investigate the interactions between membranes containing ternary mixtures of saturated lipids, unsaturated lipids, and cholesterol using the surface force apparatus (SFA). A comparison is made among measured membrane interaction force−distance profiles, vesicle zeta potential, and membrane structure/topology as determined by AFM to reveal the contributions of van der Waals, hydration, hydrophobic, and electrostatic interactions as well as subtle differences in the interactions when the fluid lipid component is singly or doubly unsaturated.

MATERIALS AND METHODS

Chemicals. 1,2-Dihexadecanoyl-*sn*-glycero-3-phosphoethanolamine (DPPE, melting point T_M = 63 °C), 1,2-dioleoyl-*sn*-glycero-3-phosphocholine (DOPC, T_M = −20 °C), 1-palmitoyl-2-oleoyl-*sn*-glycero-3-phosphocholine (POPC, T_M = −2 °C), 1,2-dipalmitoyl-*sn*-glycero-3-phosphocholine (DPPC, T_M = 41 °C), 1,2-dimyristoyl-*sn*-

Received: January 24, 2014
Revised: April 8, 2014
Published: April 9, 2014

   dx.doi.org/10.1021/la500341c | Langmuir 2014, 30, 4997−5004

glycero-3-phosphocholine (DMPC, T_M = 23 °C), 2-(4,4-difluoro-5,7-diphenyl-4-bora-3a,4a-diaza-*s*-indacene-3-pentanoyl)-1-hexadecanoyl-*sn*-glycero-3-phosphocholine (*β*-BODIPY 530/550 C_5–HPC), and cholesterol (ovine wool, >98%, T_M = 148 °C) were purchased from Avanti Polar Lipids, Inc. (Alabaster, AL) and used as received. Electrolyte solutions used $NaNO_3$ 99.995% (Sigma, St. Louis, MO). The water used was purified with a Milli-Q gradient water-purification system with a resistivity of 18 MΩ·cm.

Atomic Force Microscopy (AFM). AFM images were acquired using an MFP3D-SA system (Asylum Research, Santa Barbara, CA) with closed-loop capability. A silicon cantilever (model MSNL, Bruker, Santa Barbara, CA) with a force constant of 0.1 N/s was used for imaging. All of the images were acquired in tapping mode in Milli-Q gradient water. The cantilever was modulated by a driving frequency of 61 kHz, and the imaging set point was adjusted to 70–80% damping of the free amplitude. The AFM images were acquired and analyzed using Asylum MFP3D software developed on the Igor Pro 6.12 platform and Gwyddion version 2.33 (http://gwyddion.net/). Three independent samples for each lipid composition were scanned. The statistics of each composition were obtained from at least 100 measurements over multiple images.

Fluorescence Microscopy (FM). FM images were acquired using a Nikon Eclipse E600 microscope connected to a CoolSNAP-Pro CCD camera at 10×, 40×, and 60× magnification.

Zeta Potential Measurements (ZP). ZP was used to quantify the magnitude of the electrical charge of various membrane compositions based on measurements of vesicle mobility in an electric field in 0.45 mM $NaNO_3$ electrolyte solution (Brookhaven Zeta Plus, Holtsville, NY). Although not identical to the surface charge or surface potential determination from force profile measurements by SFA (described below), ZP provides the sign of the electrical charge and its relative magnitude referenced between the hydrodynamic shear plane at the membrane surface and the bulk solution. ZP results were obtained from at least 3 independent samples with 10 measurements per sample for each vesicle composition.

Sample Preparation. The mica-substrate-supported lipid bilayers were constructed using Langmuir–Blodgett (LB) deposition (Nima Coventry, U.K.). The inner monolayer was DPPE deposited at 45 mN/m. DPPE forms an almost defect-free, robust, strongly physisorbed monolayer on mica.[15] The dipping speed used to deposit the inner monolayer was 1 mm/min, and the monolayer transfer ratio was 0.997 ± 0.004 on freshly cleaved mica. The tight packing and stability of the gel-phase DPPE inner monolayer minimize molecular exchange between the two leaflets. The outer monolayer consisted of a 1:1:1 (mole %) mixture of either DOPC–DPPC–cholesterol or POPC–DPPC–cholesterol. Two different methods were used to deposit the outer leaflet. The main method in the reported work was to deposit the outer monolayer using a second Langmuir–Blodgett deposition. In this case, the outer leaflet was deposited at 30 mN/m with a dipping speed of 4 mm/min. The transfer ratio of the outer monolayer was 0.982 ± 0.007 for 1:1:1 DOPC–DPPC–cholesterol on DPPE and 0.983 ± 0.004 for 1:1:1 POPC–DPPC–cholesterol on DPPE. The entire process for the deposition of the outer leaflet was less than 30 min to minimize the oxidation of cholesterol and the unsaturated lipid component. Figure 1 shows the pressure–area isotherm of the mixtures used as the outer leaflet of the supported lipid bilayer. These isotherms are in agreement with the condensation effect of cholesterol on PC lipids observed by Smaby et al.[9] At 33 mol % cholesterol, the average molecular area is about 40–45 Å^2/molecule at a surface pressure of 30 mN/m.

The second method used to construct the supported membrane was vesicle fusion.[16] Lipid–cholesterol mixtures were prepared in chloroform, dried under nitrogen, and then placed under vacuum for at least 4 h. Mixtures for fluorescence microscopy imaging contained 1% bodipy-HPC. The dried lipids were hydrated with Milli-Q water to a concentration of 0.5 mg/mL, sonicated using a probe tip sonicator for 1 min, and then extruded through a 100 nm pore size polycarbonate membrane for 10 passes. Vesicle solutions for ZP were extruded and not probe tip sonicated to prevent titanium contamination. In some studies, a DPPE monolayer was incubated with the extruded vesicle solution for 1 h to create an asymmetric bilayer as in the Langmuir deposited case. In others, a freshly cleaved mica substrate was incubated with the vesicle solution to form the entire membrane by vesicle fusion. After incubation, excess vesicles were removed by extensively rinsing the sample with Milli-Q water. However, the formation of a uniform supported membrane using either vesicle fusion approach was problematic. High-resolution fluorescence microscopy and surface force measurements revealed the presence of tubules and tethered vesicles extending from the membrane surface rather than a uniform membrane. As a result, a significant repulsion was observed during the force measurements due to the confinement and compression of tubules and tethered vesicles between the supported membranes. In addition, the vesicle fusion method on either bare mica or a supported DPPE monolayer did not yield as complete membranes as demonstrated by a greater number of defects in the membranes. Furthermore, membranes formed entirely by the vesicle fusion method on a bare mica substrate were of even lower quality in terms of uniformity and surface coverage compared to membranes formed by fusion to a DPPE monolayer.

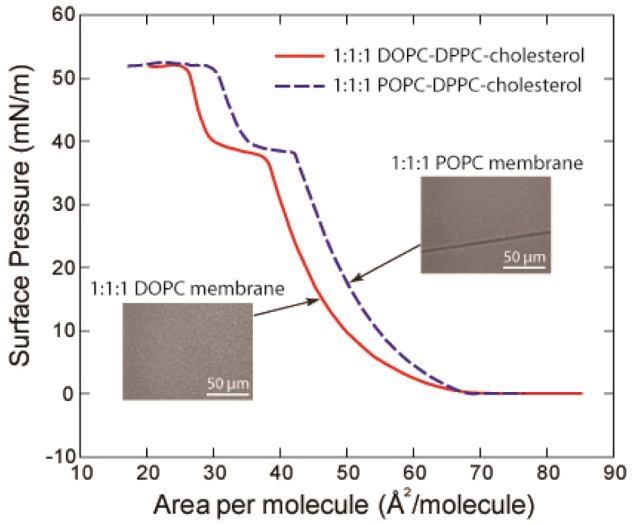

Figure 1. Isotherms of the lipid mixtures used to make the outer monolayer of the membrane bilayer at 25 °C. When both acyl chains in the fluid-phase lipid component are unsaturated (DOPC vs POPC), a larger condensation with cholesterol is observed. The top right inset is an FM image of the 1:1:1 POPC–DPPC–cholesterol membrane, and the bottom left is the FM for the 1:1:1 DOPC–DPPC–cholesterol membrane at 40× magnification. The dark stripe on the image was a scratch made to visualize the homogeneity of the membrane better.

Surface Force Measurements (SFA). The SFA technique has been used extensively to measure the interaction forces between surfaces, and details of the technique can be found in refs 17–19. On the basis of multiple-beam interferometry (MBI), the SFA provides a definitive reference for surface separation (±0.2 nm in this work). Briefly, one of the membrane-coated mica surfaces was mounted on a fixed stage, and the other was mounted on a double-cantilever spring of known stiffness (2.16 × 10^5 mN/m) which can be displaced vertically. The back of the mica substrates was coated with a 55-nm-thick evaporated silver layer. The silver layer on each disk partially transmits light directed normally through the surfaces which constructively interferes, producing fringes of equal chromatic order (FECO). The distances between the surfaces can be measured by observation of the position and displacement of FECO peak wavelengths within a spectrometer. A custom-automated SFA Mark-II was used for data collection. The system enables constant and/or variable surface displacements via a computer-controlled motor system. A sensitive CCD camera (Princeton SPEC-10:2K Roper Scientific, Trenton, NJ) was interfaced with the spectrometer and computer acquisition system to allow automated FECO wavelength

dx.doi.org/10.1021/la500341c | Langmuir 2014, 30, 4997–5004

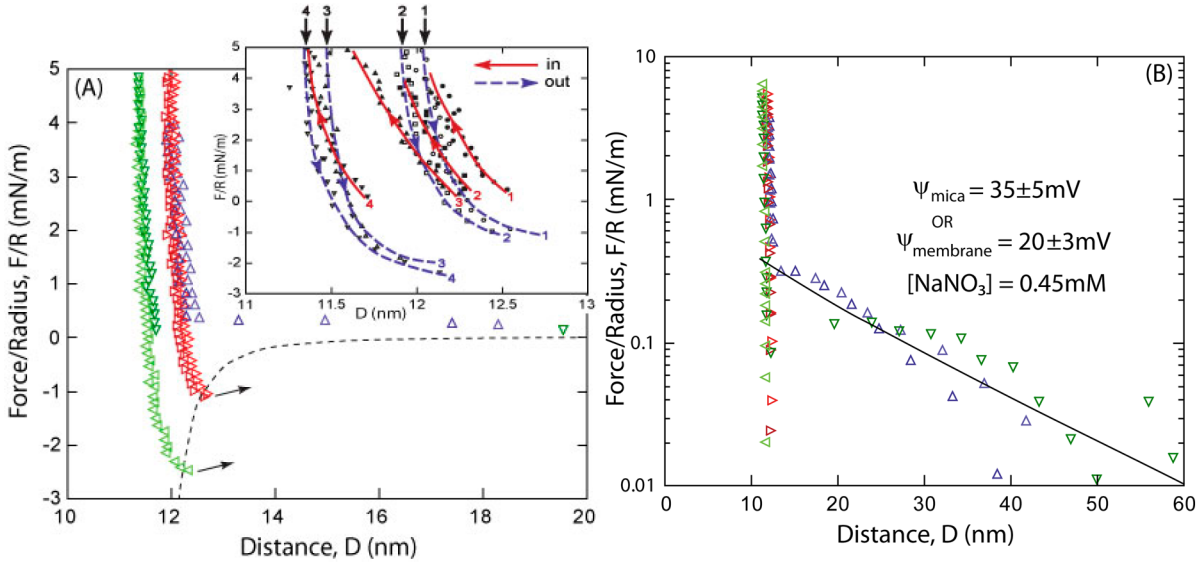

Figure 2. (A) Force−distance profiles between opposing 1:1:1 DOPC−DPPC−cholesterol in ∼0.5 mM $NaNO_3$ solution. $D = 0$ is defined as the contact between bare mica−mica surfaces. The dashed line is the predicted van der Waals interaction $F = (-AR)/(6D^2)$ with $A = 7 \times 10^{-21}$.[22] The inset shows four successively measured force profiles while allowing a longer contact time between each distance displacement. There is an inward shift to smaller separations (decreasing membrane thickness) and greater adhesion due to lipid rearrangements in the contacting region. (B) Semilogarithmic plot of the force profile and fit of the electrostatic contribution (solid line) using either the mica or membrane as the charged interface {(Δ, ∇) approach; (◁, ▷) separation}.

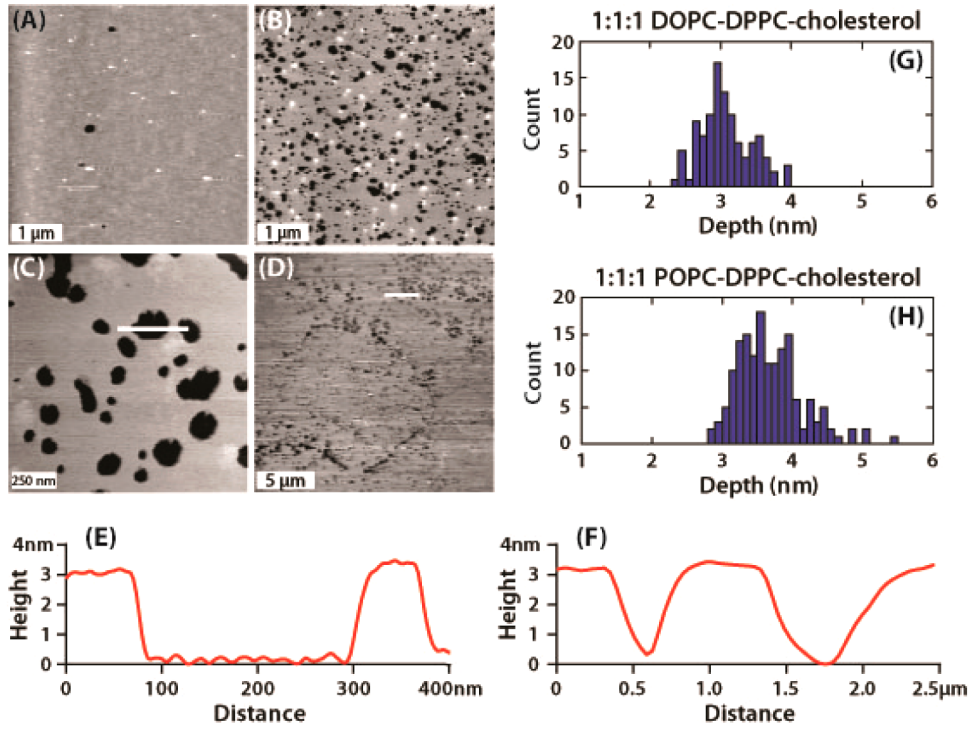

Figure 3. (A) 5 μm × 5 μm AFM topography image of the DOPC−DPPC−cholesterol system showing that there are regions that are relatively defect-free. (B) 5 μm × 5 μm AFM topography image of the DOPC−DPPC−cholesterol system showing that there are regions that have defects. (C) 1.5 μm × 1.5 μm AFM enlarged image of the DOPC−DPPC−cholesterol system with a representative cursor measuring the depth of the defect. (D) 20 μm × 20 μm AFM topography image of the POPC−DPPC−cholesterol system. (E, F) Corresponding cursor profiles as indicated in (C) and (D), respectively, to obtain defect depth profiles. (G, H) Histogram of defect depths for the DOPC−DPPC−cholesterol and POPC−DPPC−cholesterol systems, respectively.

determination. After lipid bilayer deposition, the surfaces were transferred and mounted into the SFA box under water. The water in the SFA box was saturated with 1:1:1 lipid mixtures to minimize lipid desorption from the surface during the course of the measurements. After the surfaces were mounted, the SFA box was placed in a temperature-controlled room at 25.0 °C typically overnight to allow complete equilibration. The membrane thickness was determined using the FECO wavelength shift from the membrane contact relative to the bare mica substrates after completing the experiment. Three independent SFA experiments were carried out for

dx.doi.org/10.1021/la500341c | Langmuir 2014, 30, 4997−5004

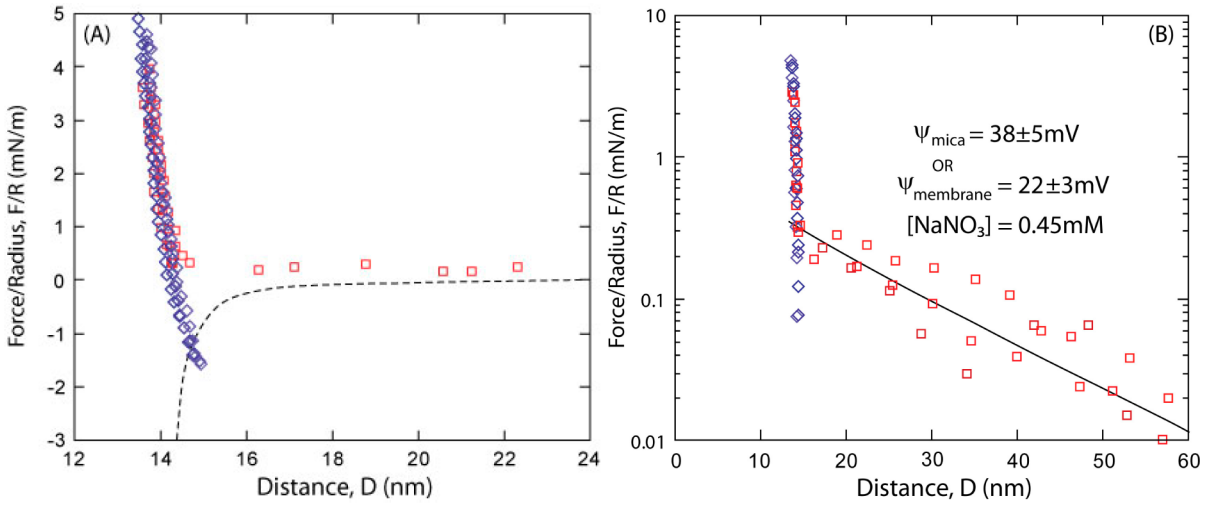

Figure 4. (A) Force–distance profiles between 1:1:1 POPC–DPPC–cholesterol membranes in ~0.5 mM $NaNO_3$ solution. $D = 0$ is defined as the contact between bare mica–mica surfaces. The dashed line is the van der Waals interaction $F = -AR/6D^2$ with $A = 7 \times 10^{-21}$ J.[22] (B) Semilogarithmic plot of the force profile and fit of the electrostatic contribution (□, approach; ◇, separation).

each of the membrane compositions. Force profiles shown in the Results section are for one set of experimental measurements but were consistent among the three independent experiments.

RESULTS

1:1:1 DOPC–DPPC–Cholesterol Membranes. Figure 2 shows the measured force–distance profile between opposing membranes with 1:1:1 DOPC–DPPC–cholesterol as the outer monolayer in 0.5 mM $NaNO_3$ solution. As the membranes were asymmetric with inner leaflets of DPPE and outer leaflets composed of mixtures of unsaturated lipid, saturated lipid, and cholesterol, we treat the two outer leaflets, which we are primarily interested in, as an equivalent membrane of the mixture composition. The force–distance profile is based on the mica–mica contact ($D = 0$ nm). The thickness of the two opposing bilayers was determined from the shift of the contact FECO wavelength before and after deposition of the bilayers on the mica substrates as well as after removal of the deposited membranes at the end of the measurements.[20] The average thickness of the two DPPE/1:1:1 bilayers was 11.7 ± 0.6 nm. The thickness of a DPPE monolayer on mica deposited at 45 mN/m has been established to be 2.56 ± 0.05 nm using the method of UV light exposure.[15,21] Therefore, the thickness of a single outer, 1:1:1 DOPC–DPPC–cholesterol monolayer including the hydration layer is ~3.3 ± 0.7 nm.

Figure 2B displays the data on a semilog plot to aid in ascertaining the source of the weak repulsive contribution to the force profile. As can be seen, the decay length of the repulsion is given by the electrolyte concentration in the solution (~0.5 mM $NaNO_3$ or $\kappa^{-1} \sim 14$ nm), indicating that the force is electrostatic. An electrostatic repulsion between the membranes was unexpected given that the membranes should be overall neutral in charge. The headgroups of PC and PE lipids are zwitterionic but neutral at pH 6, and cholesterol is not charged under these conditions. However, in the case of unsaturated lipids, there are reports that a small amount of the lipid (contaminant lipid) is charged, resulting in a weakly charged membrane. In the absence of other charges in the system, the effect of these lipid contaminants can be measurable as observed here.[23,24]

On the other hand, the underlying mica substrate is also negatively charged. AFM images of a representative and identically prepared 1:1:1 DOPC–DPPC–cholesterol membrane are shown in Figure 3A–C. As can be seen, membrane defects (which reach the underlying DPPE monolayer) are present although the membrane appears to be homogeneous under fluorescence microscopy imaging (Figure 1, bottom left inset). Figure 3E is a representative profile across a defect. The average depth of the defects was 3.0 ± 0.4 nm (Figure 3G), which is in very good agreement with the thickness of the outer monolayer as measured by SFA (3.3 ± 0.7 nm). Similar defects were previously observed on solid-supported, one-component bilayer systems using AFM at low deposition pressure.[21] Holes in the membrane, which span to the mica surface, were present but at a much smaller fraction, precluding a definitive measure of the total membrane thickness by AFM. Thus, the electrostatic repulsion measured between the opposing membranes could arise from two different sources: (1) charged lipid contaminants in the membrane or (2) exposed regions of the negatively charged mica substrates. The Poisson–Boltzmann (P–B) equation was used to fit the electrostatic contribution to the force profile for both scenarios. Assuming the origin of charge was at the mica substrate, the best electrostatic fit was obtained for a salt concentration of 0.45 mM with a surface charge of 1.8 mC/m^2 or a surface potential of 35 mV. If the origin of the charge was instead at the membrane interface, then a lower charge density of 1 mC/m^2 or a surface potential of 20 mV is obtained. The slightly lower salt concentration used in the electrostatic fit (0.45 vs 0.50 mM) is due to dilution during the transfer of the membrane-coated substrates from the Langmuir trough to the SFA.

Upon separation of the membranes, a substantial adhesion was measured. The magnitude of the adhesion with 1:1:1 DOPC–DPPC–cholesterol membranes ranged from −1.1 to −2.5 mN/m as shown in Figure 2A (arrows). A Hamaker constant of 7×10^{-21} J was used as previously determined by Marra and Israelachvili[25] to estimate the van der Waals contribution (dashed curve with the vdW plane located at $D =$ 11.5 nm). The measured adhesion between the two membranes is comparable to the prediction, but the magnitude of the adhesion is actually significantly greater than predicted once the

dx.doi.org/10.1021/la500341c | Langmuir 2014, 30, 4997–5004

repulsive electrostatic contribution is accounted for. Effectively, the adhesion is approximately 0.3−0.4 mN/m greater in magnitude, significantly greater than the vdW prediction. The enhanced adhesion suggests that hydrophobic contributions due to defects in the membrane also contribute to the adhesion.[26] A clear signature of some hydrophobic character to the adhesion was indicated by an increase in the magnitude of the adhesion with increasing contact time and compression of the membranes. As depicted in the inset of Figure 2A (run 2 vs run 3), increased contact time allowed structural rearrangements of the membrane and an enhancement in the adhesion due to the alignment of hydrophobic defects in the opposing membranes.[27−29] The structural rearrangement can be observed from the inward shift of the contact separation distance and the thinning of membranes (Figure 2A inset). The number of defects or holes and the magnitude of force applied were insufficient to result in complete hemifusion between the membranes containing cholesterol. Previously, Benz et al.[21] reported hemifusion between single-component membranes with a high number of defects under high loads.

POPC−DPPC−Cholesterol Membranes. Figure 4 shows the measured force−distance profile between opposing membranes with 1:1:1 POPC−DPPC−cholesterol as the outer monolayer in an ∼0.5 mM $NaNO_3$ solution. The force−distance plot was based on the mica−mica contact (D = 0 nm). The average thickness of two DPPE/1:1:1 bilayers was 13.5 ± 0.6 nm, yielding a thickness of 4.2 ± 0.7 nm for a single, hydrated 1:1:1 monolayer containing POPC. AFM images for the 1:1:1 POPC−DPPC−cholesterol membrane (Figure 3D) also demonstrated that defects and holes were present in membranes similar in size to the 1:1:1 DOPC−DPPC−cholesterol system. Figure 3F is a representative profile across a defect. The average depth of the monolayer defects was 3.6 ± 0.4 nm (Figure 3H), consistent with the thickness of the 1:1:1 POPC−DPPC−cholesterol monolayer obtained via SFA measurements.[30]

Fluorescence imaging of the 1:1:1 POPC−DPPC−cholesterol membrane mixture revealed a macroscopically uniform membrane, as was the case with the doubly unsaturated DOPC−DPPC−cholesterol mixture. An electrostatic repulsion was also observed, detectable from a distance of about 50 nm from the bilayer−bilayer contact. The electrostatic repulsion for this membrane composition was very similar to that obtained with the doubly unsaturated DOPC−DPPC−cholesterol membrane. With the origin of charge at the mica surface, a constant surface charge of 2 mC/m^2 or a surface potential of 38 mV was obtained. If the origin of charge was at the membrane interface due to the inclusion of a small level of charged lipids in the membrane, then a lower value of 1.1 mC/m^2 or 22 mV was obtained. Finally, the magnitude of the membrane adhesion, about −1.6 mN/m, was similar to that measured between membranes with doubly unsaturated DOPC−DPPC−cholesterol. The magnitude of the adhesion is again greater than the predicted van der Waals attraction between the membranes (vdW plane at D = 13.7 nm). In the case of POPC−DPPC−cholesterol membranes, longer contact times did not result in a significant change in the force profile or a decrease in membrane thickness due to lipid rearrangements ($\Delta D \leq 5$ nm).

DISCUSSION

Electrostatics. The general features of the measured interaction force−distance profiles of the two membrane compositions are quite similar. In both cases, a long-range but weak electrostatic repulsion was measured with a short-range, predominantly van der Waals attraction resulting in adhesion of the membranes at contact. We first discuss the electrostatic repulsion. Previous measurements of single-component membranes on mica have indicated that saturated PC and PE lipids form relatively defect-free, uncharged supported membranes on mica.[29] The ionization constant or pK_a of PC and PE lipids[31−33] at the experimental pH of ∼6 also suggests an overall neutral charge for PC and/or PE membranes.[34] In contrast, unsaturated lipids have been reported to contain a small amount of a charged, contaminant lipid that renders the membrane weakly charged.[23] With the origin of charge at the membrane interface, the resulting 1 mC/m^2 charge density corresponds to about 1 charge per 400 lipids for both 1:1:1 membrane compositions. If the origin of charge is at the mica surface due to membrane-spanning holes, then the measured surface charge density of about 2 mC/m^2 corresponds to 1 negative charge per 80 nm^2. In comparison, the basal plane of mica has a much greater negative charge of about 1 per 5 nm^2.[35] Thus, the underlying mica substrate is relatively well screened by the membrane. AFM scans of the membranes reveal that most of the features are monolayer defects (depth <3.6 nm) and not membrane-spanning holes. This finding strongly suggests that charged lipid impurities are the dominant source of electrostatic repulsion. In the case of defects, the underlying mica substrate is still coated with a DPPE monolayer. The low dielectric constant of the inner DPPE monolayer ($\epsilon \approx 3-5$) greatly inhibits charge dissociation and screens any charge at the mica surface.

To establish unequivocally that charged lipid contaminants were present in the membrane, zeta potential measurements were carried out with various compositions of POPC, DOPC, DPPC, DMPC, and cholesterol containing vesicles. Table 1 reports the measured zeta potential for the various compositions in 0.45 mM $NaNO_3$ solution to match the SFA force profile measurements. The zeta potential of the 1:1:1 compositions was −15 to −20 ± 5 mV, consistent with the SFA measurements of an electrostatic charge being present in the membrane. To establish the source of the negatively charged lipid contaminant, a variety of mixtures were studied. In all cases, the vesicles were negatively charged. The zeta potential for pure saturated lipid vesicles was measured using DMPC to enable room-temperature measurements (DMPC, T_M = 23 °C). The higher melting temperature of 41 °C for DPPC

Table 1. Summary of Zeta Potentials of Various Lipid Compositions

lipid	solution	ψ (mV)
pure DMPC	0.45 mM $NaNO_3$	−7.1 ± 4.5
pure DMPC	water	−22.3 ± 4.3
pure DOPC	0.45 mM $NaNO_3$	−10.1 ± 5.4
pure DOPC	water	−21.8 ± 4.0
pure POPC	0.45 mM $NaNO_3$	−10.9 ± 4.9
2:1 DOPC−cholesterol	0.45 mM $NaNO_3$	−12.1 ± 4.7
2:1 DOPC−cholesterol	water	−21.8 ± 4.6
2:1 POPC−cholesterol	0.45 mM $NaNO_3$	−13.9 ± 4.5
2:1 DPPC−cholesterol	0.45 mM $NaNO_3$	−10.6 ± 4.1
1:1:1 DOPC−DPPC−cholesterol	0.45 mM $NaNO_3$	−14.9 ± 4.5
1:1:1 DOPC−DPPC−cholesterol	Water	−24.2 ± 4.5
1:1:1 POPC−DPPC−cholesterol	0.45 mM $NaNO_3$	−19.5 ± 5.4

dx.doi.org/10.1021/la500341c | Langmuir 2014, 30, 4997−5004

requires that the vesicle solution temperature be maintained above T_M throughout the course of the zeta potential measurement. The difference in the length of the acyl chains should not affect the charge of the vesicle. The findings suggest that charged lipid contaminants are present in both saturated and unsaturated lipid samples. Moreover, zeta potential measurements of the surface potential at the hydrodynamic plane of the 1:1:1 vesicles were in good agreement with the SFA-measured force profiles between supported 1:1:1 membranes.

Adhesion. We now discuss the differences in adhesion between the two membrane compositions. As detailed in the Results section, the adhesion between the 1:1:1 DOPC-containing membranes varied from −1.1 to −2.5 ± 0.3 mN/m and the adhesion of 1:1:1 POPC-containing membranes was about −1.6 ± 0.2 mN/m. Although we believe hydrophobic nanoscale defects in the outer 1:1:1 monolayer are the source of the enhanced adhesion over vdW, we also consider the effect of cholesterol and potential differences in membrane hydration for completeness. Cholesterol is known to induce a "condensation effect" on various PC membranes which increases the lateral interaction between the components. Huang and Feigenson[36] suggested that the PC lipid headgroups shield the adjacent hydrophobic body of cholesterol to create an umbrella structure. Since the van der Waals plane of a predominantly lipid membrane is expected to be located at the plane of the lipid headgroups and the membrane mixtures have only one phase, the umbrella model suggests similar Hamaker constants for PC membranes with or without cholesterol. As both membranes had PC lipids and cholesterol in the same ratios, our expectation was to measure a similar adhesion between the two membrane compositions. Moreover, as PC lipids were the predominant constituent of both membranes, we further expected that the measured adhesion would be similar to previous measurements of van der Waals adhesion between pure PC membranes.

Marra and Israelachvili[25] measured and reported that the vdW adhesion between fluid-phase DMPC and DPPC membranes was about −0.6 mN/m and extracted a Hamaker constant of $A = 7 \pm 1 \times 10^{-21}$ J based specifically on measurements of DPPE and DPPC membranes. In both cases, the membrane was LB deposited presumably on an inner leaflet of DPPE as in our studies. Subsequent studies found similar values for pure DPPC membranes[37] and for DMPC on DPPE,[29] confirming this adhesive range. Conversely, the measured vdW adhesion between phosphotidylethanolamine membranes in the gel phase is significantly greater (−5 mN/m).[25] As the Hamaker constant for PC and PE lipids should be very similar, Marra and Israelachvili[25] suggested that the difference in adhesion was due to differences in the level of hydration and contact separation between the membranes, where $(F_{vdW})/R = -A/(6\pi D^2)$ and $D = 0$ corresponds to the van der Waals plane of origin which varies for different lipids based on their hydration.[38] Refractive index measurements of DPPC and DPPE monolayers also support that their Hamaker constants are within 10%.[15] Thus, variations in membrane hydration due to cholesterol, lipid composition, and/or the van der Waals plane of origin could potentially account for the differences in the measured adhesion in this work.

Due to the significant dependence on hydration, we next comment on the 0.9 nm difference in thicknesses of the 1:1:1 POPC−DPPC−cholesterol membrane versus the 1:1:1 DOPC−DPPC−cholesterol membrane as measured by SFA. In SFA experiments, the wavelength shift of the FECO fringes before and after removing the membranes was used to determine the average membrane thickness over the ∼20 × 10 μm^2 contact region. Defects or holes in the membrane below a few micrometers in lateral dimension are not resolvable, and only an average measure of the membrane thickness can be obtained. In addition, the water of hydration of the headgroups is intrinsically part of the membrane thickness. As the ratio of fluid lipid to saturated lipid to cholesterol and deposition pressure were maintained between the two membrane compositions, the difference in thickness is due to packing differences of these tricomponent mixtures with doubly or singly unsaturated acyl chains in the fluid-phase lipid (DOPC vs POPC), including any present defects or holes and any intrinsic difference in hydration, if present. With regard to packing in the mixtures, cholesterol is known to have a condensing effect on fluid-phase lipids and conversely to change solid-phase lipids, here DPPC, to fluids. Molecular dynamic simulations by Pitman and co-workers[13] have also indicated that cholesterol has a higher affinity for saturated versus unsaturated acyl chains due to better packing of the hydrophobic core. As POPC contains one more saturated acyl chain than DOPC, the POPC−DPPC−cholesterol membrane may have tighter packing, leading to an increased thickness compared to that of the DOPC-containing membrane. In contrast to this assessment, the isotherms and area per molecule measurements at the air−water interface (Figure 1) indicate that POPC-containing monolayers have a slightly higher average area per molecule than the DOPC-containing monolayers. Assuming an incompressible system, this would suggest a decrease in the thickness of the POPC-containing membrane compared to that of the DOPC containing membrane. However, isotherm measurements may not be sensitive to differences in hydration or molecule protrusions out of the membrane plane which affect the overall thickness. Thickness measurements of multicomponent lipid mixtures should be able to resolve these differences, especially if they are of substrate-supported membranes. Our AFM measurements of the two membrane compositions are consistent with an increase in thickness of the POPC-containing membrane, but only by ∼0.6 nm versus 0.9 nm by SFA. Rawicz et al.[39] showed that vesicles have very similar bending moduli for lipid mixtures of two unsaturated, two saturated, and mixed-saturation acyl chain lipids with similar chain lengths. Although bending rigidity is not a direct measure of protrusions out of the membrane plane, the similarity in the compressibility of the membrane as measured by SFA suggests that any difference in thickness due to lipid protrusions out of the membrane plane between the two membrane compositions would be very modest. Although we cannot rule out an increase in vdW adhesion due to subtle changes in hydration and lipid packing in membranes containing cholesterol, we believe the primary cause is increased hydrophobic attraction as detailed below.

In support of hydrophobic interactions as the main cause of the increased adhesion and variation in membrane thickness in the mixed membrane systems, AFM scans indicated that there were defects in both membrane mixtures which exposed the inner DPPE monolayer of the membrane. Although the levels of defects in the two mixtures were relatively similar, there was significant variation in the number of defects across the membrane, especially in the case of the 1:1:1 DOPC-containing membrane which showed a greater variation in the magnitude of the adhesion. Defects which exposed regions of the inner

dx.doi.org/10.1021/la500341c | Langmuir 2014, 30, 4997−5004

leaflet would lead to an additional hydrophobic interaction between the two membranes. These defects were relatively few in number, as hemifusion between the two membranes was not observed. Instead, the presence of defects is reflected by a decrease in the average membrane thickness in the SFA measurements which was averaged over about 100 μm^2 areas. Furthermore, in the case of 1:1:1 DOPC membranes, lipid membrane restructuring was observed with an increase in contact time (Figure 2A inset). The role of hydrophobic interactions between membranes has been well documented by Helm et al.,[27] who showed a linear increase in adhesion with decreasing lipid density in the outer membrane leaflet. Taken together, the data and analysis strongly suggest that the increased adhesion in these mixed-lipid systems primarily arises from membrane defects and their hydrophobic contributions.[40]

■ CONCLUSIONS

The interactions between lipid membranes include electrostatics, van der Waals, hydration, hydrophobic, and, in free-standing systems, significant protrusion/undulation repulsion. A large body of work has focused on recapitulating complex membrane behavior with greatly simplified systems. In particular, substrate-supported membrane systems are used extensively due to their ease of handling, compatibility of study with numerous surface-sensitive techniques, and potential applications in biotechnology and biosensing. In this work, the force profiles between 1:1:1 DOPC−DPPC−cholesterol membranes and also between 1:1:1 POPC−DPPC−cholesterol membranes were measured using SFA and were coupled to structural and chemical information to highlight the presence of lipid contaminants and the role of defects in dictating the resulting interactions. The membranes were found to carry a distinct and non-negligible negative charge due to the presence of lipid contaminants resulting in long-range electrostatic repulsion. In contact, an increase in adhesion between membranes containing cholesterol compared to a pure PC membrane was observed. The greater-than-expected adhesion was attributed to hydrophobic interactions between membrane defects. The presence of an unexpected membrane charge and membrane defects could be important in other supported membrane studies and biosensor applications where the selective binding of ligands or proteins to membranes is important.

■ AUTHOR INFORMATION

Corresponding Author

*E-mail: tlkuhl@ucdavis.edu.

Notes

The authors declare no competing financial interest.

■ ACKNOWLEDGMENTS

This work was supported by the NSF chemistry division through grant CHE-0957868. N.-N.Y. was supported by the NSF (CHE-0809977 and DMR-1104260). We thank Daniel Kienle for assistance with MMM modeling, Emily Parry for assistance with zeta potential measurements, and Easton Groves and William Chan for assistance with fluorescence microscopy measurements.

■ REFERENCES

(1) Jurak, M. Thermodynamic Aspects of Cholesterol Effect on Properties of Phospholipid Monolayers: Langmuir and Langmuir-Blodgett Monolayer Study. *J. Phys. Chem. B* **2013**, *117* (13), 3496−3502.

(2) Almeida, P. F. F. Thermodynamics of lipid interactions in complex bilayers. *Biochim. Biophys. Acta: Biomembranes* **2009**, *1788* (1), 72−85.

(3) Dietrich, C.; Bagatolli, L. A.; Volovyk, Z. N.; Thompson, N. L.; Levi, M.; Jacobson, K.; Gratton, E. Lipid rafts reconstituted in model membranes. *Biophys. J.* **2001**, *80* (3), 1417−1428.

(4) Risselada, H. J.; Marrink, S. J. The molecular face of lipid rafts in model membranes. *Proc. Natl. Acad. Sci. U.S.A.* **2008**, *105* (45), 17367−17372.

(5) Stottrup, B. L.; Veatch, S. L.; Keller, S. L. Nonequilibrium behavior in supported lipid membranes containing cholesterol. *Biophys. J.* **2004**, *86* (5), 2942−2950.

(6) Stottrup, B. L.; Stevens, D. S.; Keller, S. L. Miscibility of ternary mixtures of phospholipids and cholesterol in monolayers, and application to bilayer systems. *Biophys. J.* **2005**, *88* (1), 269−276.

(7) Veatch, S. L.; Keller, S. L. Seeing spots: Complex phase behavior in simple membranes. *Biochim. Biophys. Acta: Mol. Cell Res.* **2005**, *1746* (3), 172−185.

(8) Wydro, P.; Knapczyk, S.; Lapczynska, M. Variations in the Condensing Effect of Cholesterol on Saturated versus Unsaturated Phosphatidylcholines at Low and High Sterol Concentration. *Langmuir* **2011**, *27* (9), 5433−5444.

(9) Smaby, J. M.; Brockman, H. L.; Brown, R. E. Cholesterols Interfacial Interactions with Sphingomyelins and Phosphatidylcholines - Hydrocarbon Chain Structure Determines the Magnitude of Condensation. *Biochemistry* **1994**, *33* (31), 9135−9142.

(10) Mills, T. T.; Huang, J. Y.; Feigenson, G. W.; Nagle, J. F. Effects of cholesterol and unsaturated DOPC lipid on chain packing of saturated gel-phase DPPC bilayers. *Gen. Physiol. Biophys.* **2009**, *28* (2), 126−139.

(11) Marsh, D. Cholesterol-induced fluid membrane domains: A compendium of lipid-raft ternary phase diagrams. *Biochim. Biophys. Acta: Biomembranes* **2009**, *1788* (10), 2114−2123.

(12) Needham, D.; Nunn, R. S. Elastic-Deformation and Failure of Lipid Bilayer-Membranes Containing Cholesterol. *Biophys. J.* **1990**, *58* (4), 997−1009.

(13) Pitman, M. C.; Suits, F.; MacKerell, A. D.; Feller, S. E. Molecular-level organization of saturated and polyunsaturated fatty acids in a phosphatidylcholine bilayer containing cholesteral. *Biochemistry* **2004**, *43* (49), 15318−15328.

(14) de Joannis, J.; Coppock, P. S.; Yin, F. C.; Mori, M.; Zamorano, A.; Kindt, J. T. Atomistic Simulation of Cholesterol Effects on Miscibility of Saturated and Unsaturated Phospholipids: Implications for Liquid-Ordered/Liquid-Disordered Phase Coexistence. *J. Am. Chem. Soc.* **2011**, *133* (10), 3625−3634.

(15) Kienle, D. F.; De Souza, J. V.; Watkins, E. B.; Kuhl, T. L. Thickness and Refractive Index of DPPC and DPPE Monolayers by Multiple-Beam Interferometry. *Anal. Bioanal. Chem.*, submitted for publication.

(16) Mingeot-Leclercq, M. P.; Deleu, M.; Brasseur, R.; Dufrene, Y. F. Atomic force microscopy of supported lipid bilayers. *Nat. Protoc.* **2008**, *3* (10), 1654−1659.

(17) Israelachvili, J. N.; Adams, G. E. Measurement of Forces between Two Mica Surfaces in Aqueous-Electrolyte Solutions in the Range 0−100 nm. *J. Chem. Soc., Faraday Trans. 1* **1978**, *74*, 975−1001.

(18) Israelac, J. Thin-Film Studies Using Multiple-Beam Interferometry. *J. Colloid Interface Sci.* **1973**, *44* (2), 259−272.

(19) Kuhl, T. L.; Leckband, D. E.; Lasic, D. D.; Israelachvili, J. N. Modulation of Interaction Forces between Bilayers Exposing Short-Chained Ethylene-Oxide Headgroups. *Biophys. J.* **1994**, *66* (5), 1479−1488.

(20) Typically, the thickness of the outer membrane leaflets is determined by draining the water from the SFA, which strips off the outer leaflet monolayers. In the case of 1:1:1 mixtures, we found that some of the DPPE inner leaflet was also removed. As a result, SFA measurements were referenced to the contact of the bare mica substrates.

(21) Benz, M.; Gutsmann, T.; Chen, N. H.; Tadmor, R.; Israelachvili, J. Correlation of AFM and SFA measurements concerning the stability of supported lipid bilayers. *Biophys. J.* **2004**, *86* (2), 870−879.
(22) The van der Waals interaction was calculated using a Hamaker constant of $A = 7 \times 10^{-21}$ J and placing the van der Waals plane about 0.7 nm inward from the membrane contact at zero force. The shift of 0.7 nm was estimated from data on DPPC membranes by Marra and Israelachvili.[25]
(23) Pincet, F.; Cribier, S.; Perez, E. Bilayers of neutral lipids bear a small but significant charge. *Eur. Phys. J. B* **1999**, *11* (1), 127−130.
(24) Hemmerle, A.; Malaquin, L.; Charitat, T.; Lecuyer, S.; Fragneto, G.; Daillant, J. Controlling interactions in supported bilayers from weak electrostatic repulsion to high osmotic pressure. *Proc. Natl. Acad. Sci. U.S.A.* **2012**, *109* (49), 19938−19942.
(25) Marra, J.; Israelachvili, J. Direct Measurements of Forces between Phosphatidylcholine and Phosphatidylethanolamine Bilayers in Aqueous-Electrolyte Solutions. *Biochemistry* **1985**, *24* (17), 4608−4618.
(26) Given the absence of a long-range hydrophobic interaction in the measured force profiles, variation in the defect depth, and the absence of air bubbles, both AFM and SFM measurements suggest that there is some lipid coverage or a less-dense lipid monolayer in the defects.
(27) Helm, C. A.; Israelachvili, J. N.; Mcguiggan, P. M. Molecular Mechanisms and Forces Involved in the Adhesion and Fusion of Amphiphilic Bilayers. *Science* **1989**, *246* (4932), 919−922.
(28) Safran, S. A.; Kuhl, T. L.; Israelachvili, J. N. Polymer-induced membrane contraction, phase separation, and fusion via Marangoni flow. *Biophys. J.* **2001**, *81* (2), 659−666.
(29) Kuhl, T.; Guo, Y. Q.; Alderfer, J. L.; Berman, A. D.; Leckband, D.; Israelachvili, J.; Hui, S. W. Direct measurement of polyethylene glycol induced depletion attraction between lipid bilayers. *Langmuir* **1996**, *12* (12), 3003−3014.
(30) To minimize the contribution from the sparse holes, all of the data was first averaged, yielding a defect depth of 3.6 ± 0.5 nm. Depths greater than 2σ were then excluded to obtain a monolayer defect depth of 3.6 ± 0.4 nm.
(31) Moncelli, M. R.; Becucci, L.; Guidelli, R. The Intrinsic pK(a), Values for Phosphatidylcholine, Phosphatidylethanolamine, and Phosphatidylserine in Monolayers Deposited on Mercury-Electrodes. *Biophys. J.* **1994**, *66* (6), 1969−1980.
(32) Tsui, F. C.; Ojcius, D. M.; Hubbell, W. L. The Intrinsic Pka Values for Phosphatidylserine and Phosphatidylethanolamine in Phosphatidylcholine Host Bilayers. *Biophys. J.* **1986**, *49* (2), 459−468.
(33) Marsh, D. *CRC Handbook of Lipid Bilayers*; CRC Press: Boca Raton, FL, 1990.
(34) The pK_a of the phosphate group on PC and PE lipids is about 1, and the pK_a of the amine group on the PE lipid is around 10. The pH of the Milli-Q water used for the experiment is 6. At this pH, 99.999% of phosphate groups are deprotonated and amine groups are protonated, resulting in an overall charge of neutral for both PC and PE membranes.
(35) Guven, N. Crystal-Structures of 2m1 Phengite and 2m1Muscovite. *Z. Kristallogr. Krist.* **1971**, *134* (3−4), 196−212.
(36) Huang, J. Y.; Feigenson, G. W. A microscopic interaction model of maximum solubility of cholesterol in lipid bilayers. *Biophys. J.* **1999**, *76* (4), 2142−2157.
(37) Orozco-Alcaraz, R.; Kuhl, T. L. Interaction Forces between DPPC Bilayers on Glass. *Langmuir* **2013**, *29* (1), 337−343.
(38) Mahanty, J.; Ninham, B. W. *Dispersion Forces*; Academic Press: London, 1976.
(39) Rawicz, W.; Olbrich, K. C.; McIntosh, T.; Needham, D.; Evans, E. Effect of chain length and unsaturation on elasticity of lipid bilayers. *Biophys. J.* **2000**, *79* (1), 328−339.
(40) Hydrophobic mismatch is another factor that would contribute to the hydrophobic interaction. Equimolar compositions were primarily chosen to remain in the one-phase region of the phase diagram at room temperature. This simplifies the characterization of the membrane and the analysis of the force profiles by minimizing the contribution of hydrophobic mismatch due to membrane domains. FM and AFM experiments verified that only one phase exists for the studied composition.